Proceedings of the Estonian Academy of Sciences,
2015, **64**, 3S, 361–367
doi: 10.3176/proc.2015.3S.06
Available online at www.eap.ee/proceedings

NONLINEAR WAVES

Shock wave propagation in nonlinear microstructured wool felt

Anatoli Stulov[a*] and Vladimir Erofeev[b]

[a] Institute of Cybernetics at Tallinn University of Technology, Akadeemia tee 21, 12618 Tallinn, Estonia
[b] Mechanical Engineering Research Institute, IPM RAN, 85 Belinskogo Str., 603024 Nizhny Novgorod, Russia

Received 8 December 2014, accepted 30 March 2015, available online 28 August 2015

Abstract. On the basis of experimental data from the piano hammers study a one-dimensional constitutive equation of wool felt material is proposed and used to study compression pulse propagation in microstructured felt. One-dimensional strain wave propagation in wool felt is considered. It is revealed that stiffness of microstructured wool felt is a nonlinear function of the felt compression, and it is strongly determined by the rate of the felt loading. This means that the speed of the compression wave that propagates in such medium depends on the form of the wave and its amplitude. It is shown that a pulse of a smooth form that has no discontinuity on its front propagates with a constant speed up to the moment when the accumulation of nonlinear effects results in the eventual continuous wave breaking. After that moment, a shock wave will be formed, and the velocity of the shock wave propagation depends on the value of its amplitude jump discontinuity across the wave front. It is shown that the front velocity of the shock wave is greater than the velocity of sound in a linear medium.

Key words: medium with microstructure, wool felt properties, strain waves, shock wave propagation.

1. INTRODUCTION

The problem considered in this paper was originated by a piano hammer study. There are many papers devoted to the process of piano string excitation by the hammer impact. Here we can recollect the remarkable historical reviews by Hall [1], Suzuki and Nakamura [2], and Fletcher and Rossing [3].

It is well known [4] that the mode energy spectrum of a vibrating string may be expressed entirely through the contact time duration t_0 and the acting force $F(t)$ according to

$$A_n + jB_n = j\left[\frac{2\sin(n\pi\nu)}{n\pi c\mu}\right]\int_{-\infty}^{t_0} F(t)e^{j\omega_n t}dt. \tag{1}$$

Here A_n and B_n are Fourier amplitudes, μ is the string density, c is the speed of transverse waves, ν denotes the position of the striking point, ω_n are the normal mode frequencies, and the force history $F(t)$ can be determined from the hammer compression. This result gives the basis for a statement that the sound generated by excited string strictly depends on the interaction time between the hammer and the string, and therefore, the contact time duration t_0 is one of the most important characteristics of sound formation.

The problem of the contact time duration between the hammer and the string, as well as the discussion what can cause the hammer to rebound, is a central point of many papers (e.g. [4,5]). This problem is clarified in [6], where using the nonlinear hysteretic hammer model it was shown [7,8] that the bulk bass

* Corresponding author, stulov@ioc.ee

hammer, which is relatively light compared to the string mass, may lose the contact with a string due to only the hammer elasticity and without the assistance of waves travelling along the string.

In this paper we will show that the hammer made of felt can leave the string due to the process of the felt unloading, which is caused by compression waves travelling inside the hammer body. According to a nonlinear hysteretic piano hammer model and in reality [9], the duration of contact between the hammer and the string decreases with the increasing of the striking velocity of the hammer. It is due to the fact that the speed of waves travelling through the hammer body increases with the growth of its amplitude.

2. PIANO HAMMER PROPERTIES AND THE FELT MODEL

Felt has been used in manufacturing piano hammers for almost two hundred years. The felt made of wool is a unique and indispensable coating matter of piano hammers. The first experimental study of compression characteristics of piano hammers was reported in [10]. Further experimental testing of piano hammers presented in [9] confirmed the main dynamical features of piano hammers: (a) the nonlinearity of the force-compression characteristics of the hammer, (b) the strong effect of the hammer velocity on the slope of the loading curve, and (c) the significant influence of hysteresis, i.e. the loading and unloading processes of piano hammer are not alike. The first dynamical model of the piano hammer that took into consideration both the hysteresis of the force-compression characteristics and their dependence on the rate of the hammer loading was presented in [7]. The derived model is based on the assumption that the hammer felt (made of wool) is a microstructured material possessing history-dependent properties, or, in other words, a material with memory.

Experimental results of the piano hammer examination at different rates of loading are displayed in Fig. 1 [9]. The numerical simulation of the piano hammer impact was provided by the dynamical hysteretic model of the piano hammer, which relates the nonlinear force $F(t)$ exerted by the hammer and the felt compression $u(t)$ in the form [7]

$$F(u(t)) = F_0 \left[u^p(t) - \frac{\gamma}{\tau_0} \int_0^t u^p(\xi) \exp\left(\frac{\xi - t}{\tau_0} \right) d\xi \right], \quad 0 \leqslant \gamma < 1. \tag{2}$$

Here the instantaneous stiffness F_0 and the parameter of nonlinearity p are the elastic parameters of the felt, and the hereditary amplitude γ and the relaxation time τ_0 are the hereditary parameters.

Figure 1 demonstrates the real features of the piano hammer: with the increasing loading the contact time diminishes and the felt stiffness increases.

To consider wave propagation in the felt material and using the results of the piano hammers study, we proposed in [11] a one-dimensional constitutive equation of the wool felt material in the form

$$\sigma(\varepsilon) = E_d \left[\varepsilon^p(t) - \frac{\gamma}{\tau_0} \int_{-\infty}^t \varepsilon^p(\xi) \exp\left(\frac{\xi - t}{\tau_0} \right) d\xi \right], \quad 0 \leqslant \gamma < 1. \tag{3}$$

Here σ is the stress, $\varepsilon = \partial u / \partial x$ is the strain, u is the displacement, the constant E_d is the dynamic Young's modulus of the felt, and p, γ, and τ_0 are the same parameters of the felt that were mentioned above. Because this approach is based on the piano hammer model, we are limited to describing only the compression wave propagation ($\varepsilon(x,t) > 0$).

From Eq. (3) we may obtain the constitutive equation for very fast felt deformation, when $t \ll \tau_0$,

$$\sigma(\varepsilon) = E_d \varepsilon^p(t), \tag{4}$$

and for very slow deformation, when $t \gg \tau_0$,

$$\sigma(\varepsilon) = E_s \varepsilon^p(t). \tag{5}$$

Here the constant $E_s = E_d(1-\gamma)$ is the static Young's modulus, and in each of these two cases the unloading of the felt occurs in the same way as the loading.

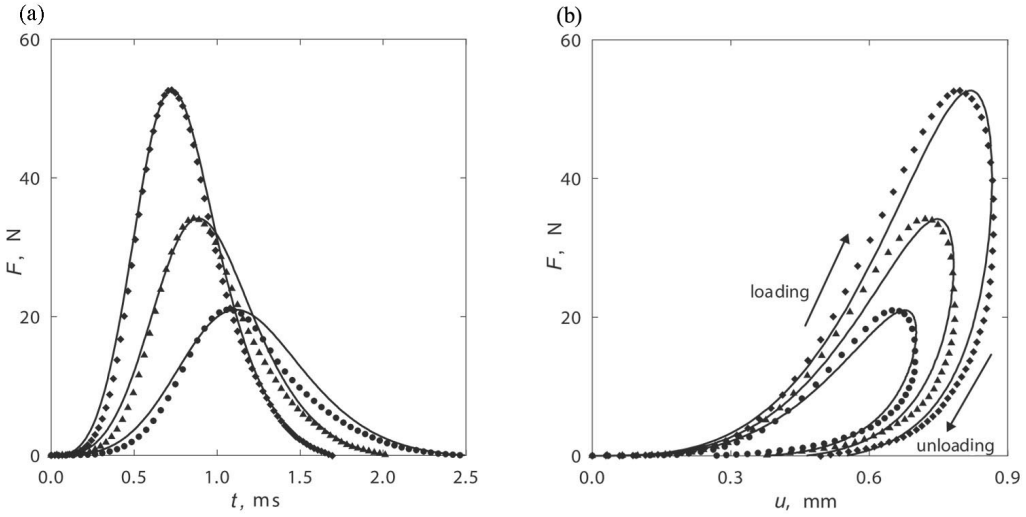

Fig. 1. Comparison of measured data and numerical simulations of piano hammers showing (a) force histories and (b) force–compression characteristics. The arrows show the directions of the compression and decompression branches. The diamonds denote measured data for hammer striking velocities 1.31 m/s (contact time $t_0 = 1.7$ ms), triangles for 1.00 m/s ($t_0 = 2.0$ ms) and bullets for 0.74 m/s ($t_0 = 2.5$ ms). The solid lines are the numerically simulated curves.

3. COMPRESSION WAVES IN FELT

The one-dimensional strain wave propagation in wool felt is considered in [11,12]. By using the classical equation of motion

$$\rho \frac{\partial^2 u}{\partial t^2} = \frac{\partial \sigma}{\partial x}, \tag{6}$$

where ρ is the felt density, and the constitutive equation (3), a nonlinear partial differential equation with third-order terms is derived in the following form [11]:

$$\rho \frac{\partial^2 u}{\partial t^2} + \rho \tau_0 \frac{\partial^3 u}{\partial t^3} - E_d \left\{ (1-\gamma) \frac{\partial}{\partial x} \left[\left(\frac{\partial u}{\partial x} \right)^p \right] + \tau_0 \frac{\partial^2}{\partial x \partial t} \left[\left(\frac{\partial u}{\partial x} \right)^p \right] \right\} = 0. \tag{7}$$

The dimensionless form of this equation is obtained by using the non-dimensional variables that are introduced by the relations

$$u \Rightarrow u/l_0, \quad x \Rightarrow x/l_0, \quad t \Rightarrow t/\alpha_0, \tag{8}$$

where

$$\alpha_0 = \tau_0/\delta, \quad l_0 = c_d \alpha_0 \sqrt{\delta}, \quad c_d = \sqrt{E_d/\rho}, \quad c_s = c_d \sqrt{\delta}, \quad 0 < \delta = 1 - \gamma \leqslant 1. \tag{9}$$

In terms of non-dimensional strain variable $\varepsilon(x,t)$ Eq. (7) reads

$$(\varepsilon^p)_{xx} - \varepsilon_{tt} + (\varepsilon^p)_{xxt} - \delta \varepsilon_{ttt} = 0. \tag{10}$$

Several samples of felt pads were subjected to static stress–strain tests. For numerical simulation the reasonable value of the static Young's modulus of felt was chosen to be $E_s = 0.1$ MPa. The value of the felt density was determined as $\rho \approx 10^3$ kg/m^3. By using the realistic values of hereditary parameters $\gamma = 0.99$ and $\tau_0 = 5$ μs presented in [9], we obtain

$$\delta = 0.01, \quad E_d = 10 \text{ MPa}, \quad c_s = 10 \text{ m/s}, \quad c_d = 100 \text{ m/s}. \tag{11}$$

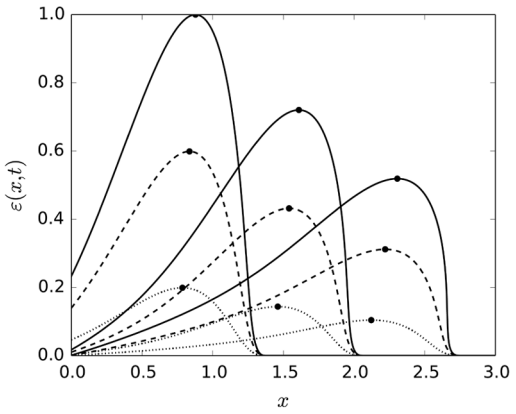

Fig. 2. Nonlinear evolution of a pulse ($t_m = 1/2$) for time moments $t = 2$, $t = 3$, and $t = 4$. Pulses of an initial amplitude $A = 0.1$ are shown by the solid lines, $A = 0.06$ by dashed lines, $A = 0.02$ by dotted lines. Bullets show the position of the pulse maximum. The results have been normalized relative to the largest amplitude ($A = 0.1$).

By using these values of material constants, the space scale l_0 and time scale α_0 that were used in (8) are

$$l_0 = 5 \text{ mm}, \quad \alpha_0 = 0.5 \text{ ms}. \tag{12}$$

Numerical analysis of the strain wave propagation is considered in [11]. This calls for the solution of the boundary value problem of Eq. (10). A boundary value of the strain prescribed at $x = 0$ is selected in the following form

$$\varepsilon(0,t) = A \left(\frac{t}{t_m} \right)^3 e^{3(1-t/t_m)}, \tag{13}$$

where t_m defines the time coordinate corresponding to the maximum of the pulse amplitude A. This form of a pulse is continuous and smooth, and it is very similar to the force history pulse shown in Fig. 1a. The front of a pulse satisfies the necessary conditions $\varepsilon(0,0) = \varepsilon_t(0,0) = \varepsilon_{tt}(0,0) = 0$.

The effect of the initial pulse amplitude A on the pulse evolution is presented in Fig. 2. The material parameters were selected as $\delta = 0.2$ and $p = 1.5$. The numerical solution is presented for three sequential time moments and for three different values of the initial amplitude A of the boundary value (13).

One can see that in this case the front velocity is a constant value $V_f = c_s$ and does not depend on the pulse amplitude. On the other hand, it is also evident that for larger amplitudes the maximum point, or the crest of a pulse (shown by bullets), propagates faster than its front.

Therefore a forward-facing slope of a pulse becomes steeper with a distance of propagation, and accumulation of this effect results finally in the pulse breaking. This means that the shock wave will be formed at the moment when the forward-facing slope of a pulse becomes vertical, and thus the value of discontinuity across the wave front is determined by the amplitude of the pulse crest.

4. SHOCK WAVE PROPAGATION

Here we consider the propagation of a pulse with a finite jump discontinuity on the front through felt material. For any rate of loading the felt material is defined with the aid of the nonlinear constitutive equation (3) in the form

$$\sigma(U) = E_d \left[(U_x)^p - \frac{\gamma}{\tau_0} \int_{-\infty}^{t} (U_x)^p \, e^{(\omega - t)/\tau_0} d\omega \right], \qquad p > 1, \qquad 0 \leqslant \gamma < 1. \tag{14}$$

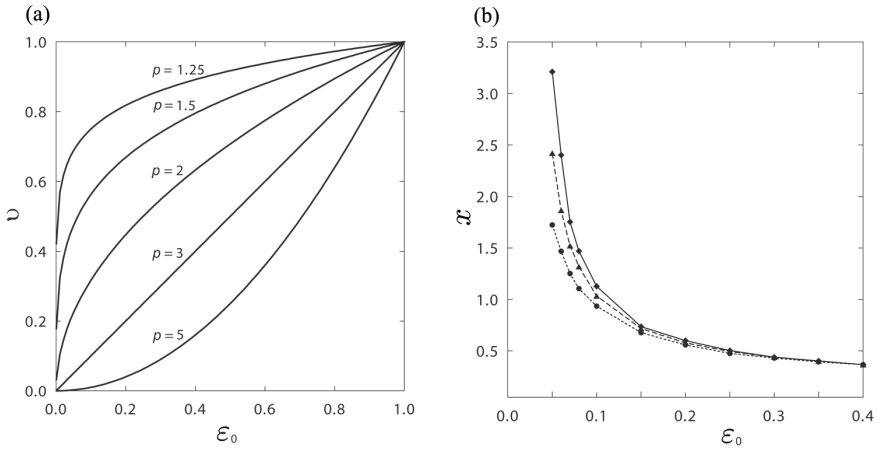

Fig. 3. Shock wave parameters as functions of the value of discontinuity ε_0 across the wave front. (a) Non-dimensional front velocity υ shown for various values of parameter p. (b) Non-dimensional distance x of the shock formation shown for $\delta = 0.01$ (diamonds), $\delta = 0.2$ (triangles), and $\delta = 0.6$ (bullets).

The conservation law

$$\frac{d}{dt}\int_{x_1}^{x_2} \rho U_{tt}(x,t)dx = \sigma(x_2,t) - \sigma(x_1,t) \tag{15}$$

gives a correspondence between the shock conditions and the shock velocity V_s

$$[\sigma] = -\rho V_s [U_t], \tag{16}$$

where the brackets indicate the jump in the quantity [13].

The constitutive equation (3) gives the relationship

$$[\sigma] = E_d [U_x]^p. \tag{17}$$

By using Eqs (16) and (17) and taking into account the kinematic identity $[U_t] = -V_s[U_x]$, one can find the relationship between the anticipated front velocity V_s and the value of the discontinuity $[U_x]$ across the wave front

$$\upsilon = \frac{V_s}{c_d} = [U_x]^{\frac{p-1}{2}}, \qquad [U_x] = [\varepsilon] = \varepsilon_0 = \text{const} > 0. \tag{18}$$

The dependence of non-dimensional front velocity on the value of discontinuity across the wave front is shown in Fig. 3a. As it was mentioned above, in the linear case and for the continuous smooth pulse ($\varepsilon_0 = 0$) the front velocity is a constant value $V_f = c_s$. In case of the shock wave propagation ($\varepsilon_0 > 0$), the front velocity V_s is always greater than V_f because $c_d > c_s$ (see relationships (9)).

By numerical simulation of the strain wave propagation, whose initial form is given by the smooth and continuous boundary value (13), the distances at which the shock pulse is formed were specified and the values of discontinuity across the wave front at these points were determined. These dependences of the distance x of the shock wave appearance as a function of the value of discontinuity ε_0 across the wave front for various values of parameter δ are presented in Fig. 3b.

5. CONCLUDING REMARKS

Resuming the results presented above, we can state that the compression wave, whose shape is initially continuous and smooth enough, propagates with a constant speed $V_f = c_s$ until the shock pulse is formed. After that moment the pulse propagates with a velocity $V_s > V_f$, and this velocity depends on the value of the discontinuity ε_0 across the wave front, which, in turn, depends on the initial wave amplitude.

Table 1. Parameters of pulse propagation

ε_0	x, 1	X, mm	t_1, ms	L_x, mm	υ, 1	V_s, m/s	t_2, ms	t_*, ms	V_{av}, m/s
0.05	3.20	16.0	1.600	0	0.473	47.3	0	1.600	10.00
0.075	1.75	8.75	0.875	7.25	0.523	52.3	0.139	1.014	15.78
0.10	1.13	5.65	0.565	10.35	0.562	56.2	0.184	0.749	21.36
0.15	0.74	3.70	0.370	12.30	0.622	62.2	0.198	0.568	28.17
0.20	0.60	3.00	0.30	13.00	0.669	66.9	0.194	0.494	32.39

Finally, using the data obtained, we can estimate the average velocity V_{av} of the compression wave propagating through the felt material. For a numerical example we have chosen the nonlinear parameter $p = 1.5$, and the distance of wave propagation $L = 16$ mm, which is equal approximately to the double thickness of the first bass piano hammer. Here we chose the same felt parameters, the space scale l_0, and the time scale α_0 as are presented in (11) and (12).

The non-dimensional parameters x and υ are obtained by using data from Fig. 3. The other parameters presented in Table 1 are determined by the relations

$$X = xl_0, \quad L_x = L - X, \quad V_s = \upsilon c_d, \quad t_1 = X/c_s, \quad t_2 = L_x/V_s, \quad t_* = t_1 + t_2, \quad V_{\mathrm{av}} = L/t_*. \tag{19}$$

Here X is the distance through which the wave propagates in a felt with a 'normal' speed c_s in the time t_1, L_x is the part of a whole distance L through which the wave propagates in the time t_2 with the velocity V_s, and t_* is the total time of propagation.

Analysis of the data displayed in Table 1 shows that the wave with a small initial amplitude, which results in the value of jump discontinuity across the wave front $\varepsilon_0 = 0.05$, propagates through the whole distance as a smooth pulse. With the increasing wave amplitude, the appearance of the shock pulse increases the average propagation speed V_{av}.

We associate here the total time of propagation t_* with the duration of contact between the hammer and the string. The amount of time decreases with the increasing of the amplitude of the hammer impact. This means that the speed of waves, travelling from the contact point to the hammer kernel and back, increases with the growth of its amplitude. Here we can state that the time of propagation t_* decreased and the average speed of propagation increased with a rise of the wave amplitude just in the similar manner as the nonlinear hysteretic piano hammer model predicts.

ACKNOWLEDGEMENTS

This research was supported by the European Regional Development Fund (Project TK124 (CENS)) and by the Estonian Ministry of Education and Research (SF 0140077s08).

REFERENCES

1. Hall, D. E. Piano string excitation III: general solution for a soft narrow hammer. *J. Acoust. Soc. Am.*, 1987, **81**, 547–555.
2. Suzuki, H. and Nakamura, I. Acoustics of pianos. *Appl. Acoust.*, 1990, **30**, 147–205.
3. Fletcher, N. H. and Rossing, T. D. *The Physics of Musical Instruments*. Springer-Verlag, New York, 1991, 319–321.
4. Hall, D. E. Piano string excitation in the case of small hammer mass. *J. Acoust. Soc. Am.*, 1986, **79**, 141–147.
5. Askenfelt, A. and Jansson, E. V. From touch to string vibrations. III: string motion and spectra. *J. Acoust. Soc. Am.*, 1993, **93**, 2181–2196.
6. Stulov, A. Piano hammer–string interaction. In *Proceedings of ICA 2004*. Kyoto, Japan, 2004, Vol. III, 2127–2130.
7. Stulov, A. Hysteretic model of the grand piano hammer felt. *J. Acoust. Soc. Am.*, 1995, **97**, 2577–2585.
8. Stulov, A. Dynamic behavior and mechanical features of wool felt. *Acta Mech.*, 2004, **169**, 13–21.
9. Stulov, A. Experimental and computational studies of piano hammers. *Acta Acust. united Ac.*, 2005, **91**, 1086–1097.

10. Yanagisawa, T. and Nakamura, K. Dynamic compression characteristics of piano hammer. *Transactions of Musical Acoustics Technical Group Meeting of the Acoustic Society of Japan*, 1982, **1**, 14–18.
11. Kartofelev, D. and Stulov, A. Propagation of deformation waves in wool felt. *Acta Mech.*, 2014, **225**, 3103–3113.
12. Kartofelev, D. and Stulov, A. Wave propagation and dispersion in microstructured wool felt. *Wave Motion*, 2015, **57**, 23–33.
13. Whitham, G. *Linear and Nonlinear Waves*. Wiley-Interscience, New York, 1974.

Lööklainete levimine mittelineaarses mikrostruktuurses villases vildis

Anatoli Stulov ja Vladimir Erofeev

On uuritud ühemõõtmelist survelainete levi villases vildis. Vilti vaadeldakse mikrostruktuurse materjalina ja selle omadusi kirjeldav olekuvõrrand on tuletatud klaverihaamritega sooritatud eksperimentidest saadud andmete põhjal. Selle järgi on vildi jäikuse ja (surve)deformatsiooni vahel mittelineaarne seos, mis omakorda sõltub tugevalt koormamise kiirusest. See tähendab, et sellises keskkonnas leviva survelaine kiirus sõltub laine kujust ja amplituudist. Autorid näitavad, et algselt katkevusi mitteomav laine levib jääva kiirusega kuni ajahetkeni, kui mittelineaarsete efektide mõju akumuleerumine viib lööklaine formeerumiseni. Tekkinud lööklaine kiirus sõltub selle amplituudist katkevuskohas ja on suurem kui heli kiirus lineaarses keskkonnas.